

## STOCHASTIC ESTIMATION OF MULTI-VARIABLE HUMAN ANKLE MECHANICAL IMPEDANCE

**Mohammad A. Rastgaar<sup>1</sup>**

rastgaar@mit.edu

**Hyunglae Lee<sup>1</sup>**

hyunglae@mit.edu

**Hermano Igo Krebs<sup>1,2,3</sup>**

hikrebs@mit.edu

**Patrick Ho<sup>1</sup>**

patrxho@mit.edu

**Neville Hogan<sup>1,4</sup>**

neville@mit.edu

<sup>1</sup>Department of Mechanical Engineering, Massachusetts Institute of Technology, Cambridge MA 02139

<sup>2</sup>Department of Neurology and Neuroscience, Weill Cornell Medical College, New York, NY 10021

<sup>3</sup>Department of Neurology, University of Maryland School of Medicine, Baltimore, MD 21201

<sup>4</sup>Department of Brain and Cognitive Sciences, Massachusetts Institute of Technology, Cambridge, MA 02139

### ABSTRACT

*This article presents preliminary stochastic estimates of the multi-variable human ankle mechanical impedance. We employed Anklebot, a rehabilitation robot for the ankle, to provide torque perturbations. Time histories of the torques in Dorsi-Plantar flexion (DP) and Inversion-Eversion (IE) directions and the associated angles of the ankle were recorded. Linear time-invariant transfer functions between the measured torques and angles were estimated for the Anklebot and when the Anklebot was worn by a human subject. The difference between these impedance functions provided an estimate of the mechanical impedance of the ankle. High coherence was observed over a frequency range up to 30 Hz, indicating that this procedure yielded an accurate measure of ankle mechanical impedance in DP and IE directions.*

### INTRODUCTION

The mechanical impedance of the human ankle plays a major role in lower extremity function during locomotion such as maintaining the upright posture, shock absorption, lower-limb joint coordination during walking, steering, and propulsion on level ground and slopes – all functions which involve mechanical interaction of the foot with the contacting surface. One method for measuring ankle impedance is stochastic perturbation. The advantage of stochastic methods over steady-state procedures is that they provide a quantitative estimate without requiring any *a-priori* assumption about the order or dynamic structure of mechanical impedance. In particular, they do not require the common assumption that impedance is composed of inertia, damping and stiffness, but are applicable to more complex, higher-order dynamics. In prior work, Kirsch et. al. [1] estimated the ankle impedance in dorsiflexion direction by superimposing small stochastic motion perturbations during a large dorsiflexion motion

of the foot. Application of position perturbations requires care to avoid applying excessive force to the subjects' joints. Van der Helm et. al. [2] used a linear hydraulic actuator to impose force perturbations for identification of intrinsic and reflexive components of the human arm [2]. In earlier work, we employed MIT-MANUS to apply pseudo-random force perturbations to estimate the mechanical impedance of the arm in two degrees of freedom simultaneously [3].

In this paper, we employed Anklebot, a rehabilitation robot for the ankle, and a similar methodology for stochastic identification of human ankle mechanical impedance. The mechanical impedance of the ankle in DP and IE were determined from nonparametric estimation of the best-fit linear transfer functions relating torques to angles in DP and IE directions. Anklebot is backdrivable with low friction and allows human subjects to move their foot freely in three degrees of freedom (DOF) relative to the shank; a detailed description can be found in [4]. Of those, two DOFs are actuated. Two nearly parallel actuators generate a dorsi-plantarflexion torque if both apply identical forces in the same direction, and inversion-eversion torque if they apply identical forces in opposite directions. As a result, the robot can apply simultaneous perturbations in two degrees of freedom of the ankle. Displacements of the linear actuators are measured by linear encoders. The ankle torques and angles were described in detail in [4] and are estimated from:

$$\tau_{dp} = (F_{right} + F_{left})x_{tr,len} \quad (1)$$

$$\theta_{dp} = \theta_{dp,offset} + \sin^{-1}\left(\frac{L_{shank}^2 + x_{tr,len}^2 - x_{link,disp}^2}{2L_{shank}x_{tr,len}}\right) \quad (2)$$

$$\tau_{ie} = (F_{right} - F_{left})x_{tr,width} / 2 \quad (3)$$

$$\theta_{ie} = \theta_{ie,offset} + \arctan\left(\frac{x_{right} - x_{left}}{x_{tr,width}}\right) \quad (4)$$

where  $\tau_{dp}$  and  $\tau_{ie}$  are the torques in DP and IE directions respectively. The other parameters in Eq.(1-4) are described in Fig.1.

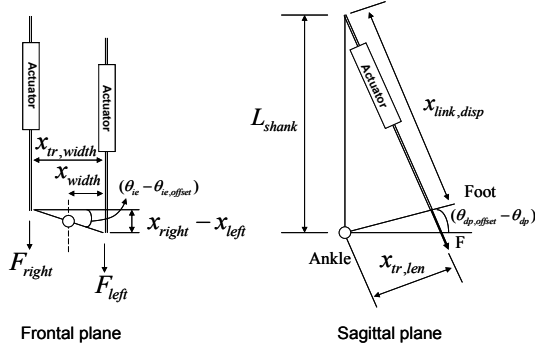


FIGURE 1. SCHEMATIC OF ANKLEBOT AND ITS GEOMETRICAL PARAMETERS

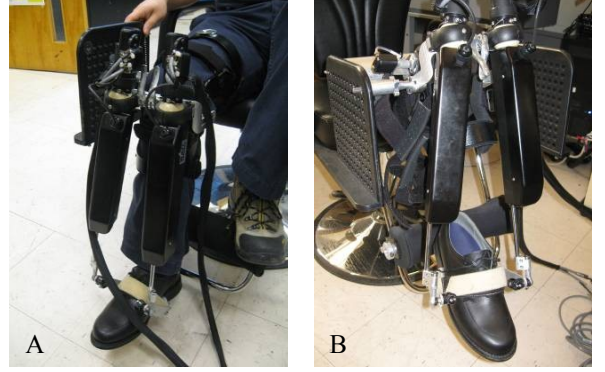


FIGURE 2. A- EXPERIMENT WITH HUMAN SUBJECT B- EXPERIMENT WITH ANKLEBOT ALONE

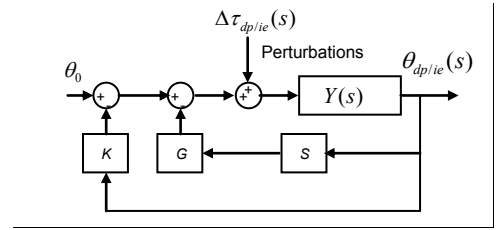


FIGURE 3. BLOCK DIAGRAM OF THE ANKLEBOT FEEDBACK CONTROL.  $Y(s)$  INCLUDES THE DYNAMICS OF ANKLE AND ANKLEBOT.

## EXPERIMENT METHODOLOGY AND RESULTS

Estimation of ankle impedance in the DP and IE directions consisted of two steps. First, two uncorrelated pseudo-random command voltages with bandwidth of 100Hz were applied to each actuator to produce torque perturbations that moved a subject's<sup>1</sup> foot in all directions in the frontal and sagittal planes while remaining within the natural limits of the joint (Fig. 2-A). The second step consisted of repeating the experiment with the hardware alone (Fig. 2-B). Each test took 60 seconds and we recorded the displacements of the actuators and the commanded voltages. We estimated the torques and angles in DP and IE directions according to Roy et al [4]. Two linear time-invariant transfer functions were then estimated in the frequency domain in each direction by computing the ratio of the cross power spectral density of angle and torque to the power spectral density of angle.

The block diagram of the system in the frequency domain is shown in Fig. 3.  $Y(s)$  is the open loop transfer function between the torque inputs and angle outputs, admittance the inverse of impedance,  $Z(s)$ .  $Y(s)$  represents the ankle and Anklebot dynamics (step 1) or the dynamics of the Anklebot alone (step 2). To maintain the neutral position of the Anklebot at almost the middle of its range of motion, we employed a PD controller. The closed-loop transfer function of the system is given in Eq. 5.

<sup>1</sup>All subjects gave their informed consent prior to testing. The protocol was approved by the Massachusetts Institute of Technology Committee on the Use of Humans as Experimental Subjects (MIT-COUHES).

$$\frac{\theta(s)_{out}}{\tau(s)_{in}} \Big|_{closed-loop} = \frac{Y(s)}{1 + (K + GS)Y(s)} \quad (5)$$

where  $\theta(s)$  is the output angle due to the input torque  $\tau(s)$ .  $K$  and  $G$  are PD controller feedback gains for position and velocity. The effect of the PD controller was removed from the data analysis as shown in Eq. 6.

$$Z(s) = Y(s)^{-1} = \frac{\tau(s)}{\theta(s)} \Big|_{closed-loop} - K - GS \quad (6)$$

Since the foot and shoe share the same motion, they can be regarded as parallel impedance elements. Ankle impedance in the DP and IE directions are the differences between step 1 and 2 in the associated directions as shown in Eq. (7).

$$Z(s) \Big|_{ankle} = Z(s) \Big|_{ankle+anklebot} - Z(s) \Big|_{anklebot} \quad (7)$$

Figure 4 shows Bode plots of the impedance magnitude and phase in the DP direction with their associated standard error. The magnitude and phase for both steps, with and without the human subject are presented. Both of the transfer functions are estimated as complex vectors and their difference is the ankle

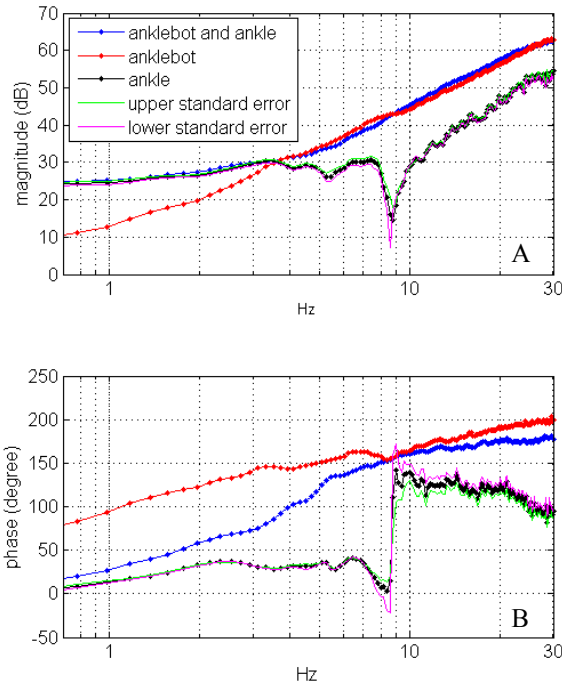


FIGURE 4. A- MAGNITUDE AND B- PHASE PLOTS OF IMPEDANCE OF ANKLEBOT WITH ANKLE, ANKLEBOT ALONE, AND ANKLE IN DP DIRECTION

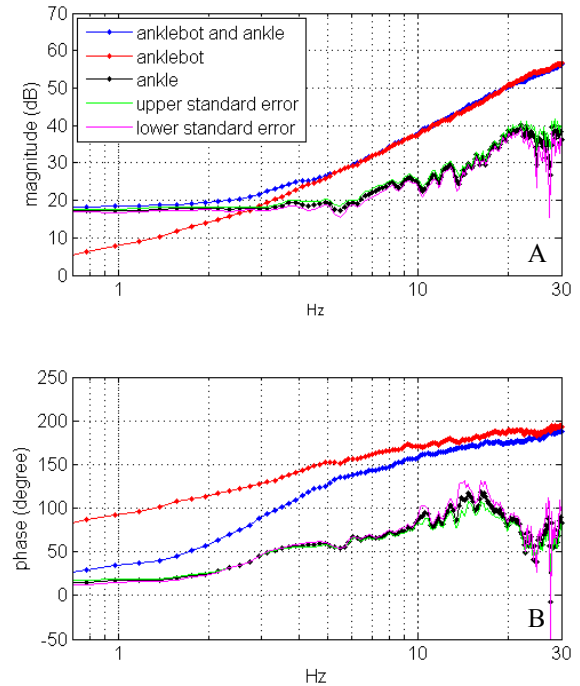


FIGURE 5. A- MAGNITUDE AND B- PHASE PLOTS OF IMPEDANCE OF ANKLEBOT WITH ANKLE, ANKLEBOT ALONE, AND ANKLE IN IE DIRECTION

impedance in the DP direction. Similar plots for ankle mechanical impedance in the IE direction are shown in Fig. 5.

## DISCUSSION

An important goal of this study was to quantify the dynamic impedance of the ankle, here presented as a function of frequency. The coherence of the linear transfer functions that describe the impedance in both the DP and IE directions were greater than 0.85 over the 0.5 to 30 Hz frequency range. Below 0.5 Hz, the coherences were relatively low, probably due to nonlinearities of the electromechanical hardware (such as friction and motor cogging). The plots of ankle impedance in DP and IE directions show that at frequencies above about 9 Hz, inertia dominates, since the magnitude plot rolls up with a slope of nearly 40 dB/decade. Below 9 Hz the stiffness of the ankle and lower extremity muscles play the dominant role. It is evident from the transition of phase angles from 0 to 180° that pass through 90° at 9 Hz. Another significant observation is that impedance in DP direction was larger than in the IE direction, which is similar to the results of static impedance tests reported elsewhere.

The results verify that multivariable stochastic estimation methods yield a reliable measure of ankle mechanical impedance in the DP and IE degrees of freedom over a relatively wide range of frequencies. Ongoing work will increase the number of experimental subjects to determine statistically reliable estimates

of ankle mechanical impedance in DP and IE directions.

## ACKNOWLEDGMENTS

The authors would like to acknowledge the support of Toyota Motor Corporation's Partner Robot Division. H. Lee is supported in part by a Samsung Scholarship.

## REFERENCES

- [1] Kirsch R. F., Kearney R. E., 1997, "Identification of time-varying stiffness dynamics of the human ankle joint during an imposed movement", *Exp Brain Res*, 114, pp. 71–85.
- [2] van der Helm F. C. T., Schouten A. C., de Vlugt E., Brouwn G. G., 2002, "Identification of intrinsic and reflexive components of human arm dynamics during postural control", *Journal of Neuroscience Methods*, 119, pp.1-14.
- [3] Palazzolo J. J., Ferraro M., Krebs H. I., Lynch D., Volpe B. T., and Hogan N., 2007, "Stochastic Estimation of Arm Mechanical Impedance During Robotic Stroke Rehabilitation", *IEEE Transactions on Neural Systems and Rehabilitation Engineering*, 15(1), March, pp. 94-103.
- [4] Roy, A., Krebs, H. I., Williams, D.J., Bever, C.T., Forrester, L.W., Macko, R.M., Hogan, N., 2009, "Robot-Aided Neurorehabilitation: A Novel Robot for Ankle Rehabilitation", *IEEE Transactions on Robotics*, 25(3), June, pp. 569-582.